CFD validation of pressure fluctuations in a pump turbine

A.G Backman, J.T. Billdal
Rainpower Norway
Gåsevikveien 6, P.O.box 144
N-2027 Kjeller, Norway

M. J. Cervantes
Luleå University of Technology,
Dep. of Applied Physics and
Mechanical Engineering,
SE-97187 Luleå, Sweden

A.R. Zobeiri, M. Farhat
École Polytechnique Fédérale de Lausanne,
Laboratory for Hydraulic Machines,
Avenue de Cour 33bis,
CH-1007 Lausanne, Switzerland

Nomenclature

C_p Pressure coefficient   [-]

$$C_p = \frac{p - \bar{p}}{{}^1\!/\!_2 \rho U_{per}^2}$$

f_r Runner rotational speed   [s^{-1}]
n_{gv} Number of guide vanes   [-]
n_{rb} Number of runner blades   [-]
f_{gv} Guide passing frequency   [s^{-1}]
$$f_{gv} = f_r \cdot n_{gv}$$
f_{rb} Runner blade passing frequency   [s^{-1}]

$$f_{rb} = f_r \cdot n_{rb}$$

H Head   [m]
Q Flowrate   [m^3/s]
n_q Specific speed

$$n_q = \frac{n\sqrt{Q}}{H^{0.75}}$$ [$s^{-3/2}$]

v Specific speed (dimensionless)
$0.035 \cdot \frac{n_q}{g^{3/4}}$ [-]

Introduction

With growing environmental awareness, power producers are turning their attention to renewable energy sources. Favourable government support has in many countries led to a dramatic increase in wind power development. This has in turn contributed to a raised need for hydro pumped storage plants to guarantee the stability of the power grids. To allow for increased reliability and operating range, manufacturers must focus on learning more about the dynamic behavior of pump turbines.

The Hydrodyna research project is a collaboration project between turbine manufacturers and Ecole Polytechnique Fédérale de Lausanne, Switzerland, which aims to improve the understanding of high head pump turbine dynamics. It is not unusual that modern pump turbines operate at heads around 500 - 700 m. For such high heads, rotor stator interaction is known to be of greater significance due to higher water velocities and smaller radial gap between the blade rows, B. Nennemann et al. [1]. The Hydrodyna research project aims to break through a technology gap in the understanding of pressure fluctuations due to rotor stator interaction.

A. Zobeiri et al. [2] presented results from simulations on the Hydrodyna geometry showing that it is possible to, within small margins of error, reproduce experimentally measured pressure fluctuations. The results focused on validation of simulated pressure fluctuations in the stator and the rotor. A. Zobeiri et al. concluded that including stay vanes is important but that including the spiral casing is not.

This work presents the results from unsteady simulations of the Hydrodyna model turbine operating at full load. In order to find the best setup, different simulations were run on guide vanes and a runner with combinations including the stay vanes and draft tube. The dynamic behavior of rotor stator interaction is visualized and examined at key frequencies on the pressure and suction side of a runner blade.

The results are validated against laboratory pressure measurements on a runner blade and Laser Doppler Velocimetry (LDV) measurements in a guide vane channel. The experimental measurements were performed within the Hydrodyna project at the Laboratory for Hydraulic Machines, EPFL.

1. Hydrodyna test case

The investigations have been carried out on the Hydrodyna model scale pump turbine in the hydraulic laboratory at EPFL in Lausanne, Switzerland. The independent test facility has a number of universal test rigs that can be set up to test different types of turbine models, such as pump turbines and turbines with axial or radial inflow.

The Hydrodyna model has a specific speed $\upsilon = 0.19$ ($n_q = 30$). The geometry consists of 20 stay vanes and guide vanes and 9 runner blades. The operational point investigated in the present work corresponds to full load turbine mode, 43% over the flow at best efficiency point. At this operational point, the guide vanes have a maximum opening and the distance between the guide vane trailing edges and the runner blade leading edges is at a minimum. This setup produces strong rotor stator interactions.

1.1 Transient pressure measurements
Static and dynamic pressure measurements are carried out at the walls of both stationary and rotating components of the pump-turbine with the help of miniature piezo-resistive sensors. 48 transducers, having 3 mm diameter, are flush mounted on the upper and lower walls of the guide vanes and stay vane channels. In the impeller, 30 similar sensors are embedded in the wall of 3 impeller blades. The specific procedure developed at EPFL to fit pressure sensors in turbine blades as well as the conditioning electronic and signal acquisition is described in [3]. The conditioning electronics are fitted in the runner crown and connected to 8 acquisition boards located in the turbine shaft. The maximum sampling frequency is 20 kHz with 12 bits A/D resolution. A 4-channels slip ring installed at the top of the turbine shaft is used to ensure power supply as well as data transmission. The transfer rate of digitized data is 1.5 Mbits/sec. The synchronization of the data sampling in both rotating and stationary frames is ensured by a tachymeter. Static as well as dynamic calibrations of the pressure sensors are carried out as described in [3]. The static calibration of the pressure transducers is performed in a pressurized tank. The voltage outputs are averaged and compared to the readings of a high precision pressure transducer used as a reference. The measurement error is less than 0.5% of the measurement range. To resolve the problem of zero drift, the test rig is systematically shut down every 30 minutes to reset the transducers offsets.

The rotor stator interaction was measured as pressure fluctuations on the pressure and suction side of one rotor blade as shown in figure 1. The results are been presented in figure 2. The pressure values are normalized with respect to the runner peripheral velocity C_p.

The amplitude is greatest at the leading edge of the blade and faded further into the runner blade channel. The guide vane passing frequency, $f_{gv} = 326.66$ Hz can be seen with two harmonies.
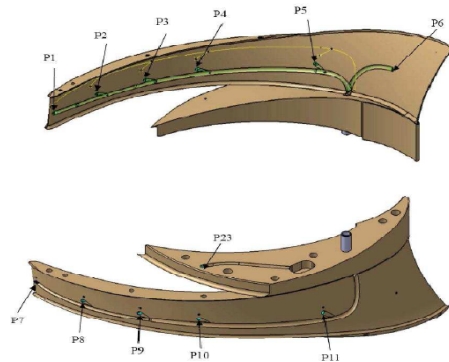

Fig. 1. The pressure transducer chambers as seen from the inside of the blade, before mounting. Pressure transducers 1-6 registering the pressure side and transducers 7-11 registering the suction side of the blade. Figure from B. Nennemann and T.C. Vu, [4].
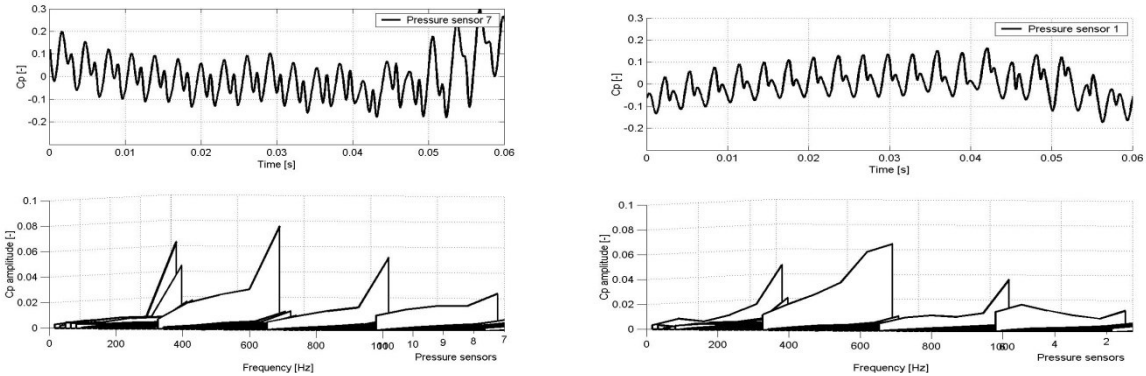
Fig. 2. Pressure fluctuations on the suction and pressure side, leading edge and waterfall plots.

1.2 LDV measurements

The velocity survey in the pump turbine is carried out by a Laser Doppler Velocimeter (LDV). This non intrusive instrument uses an Ion-Argon laser source (COHERENT, model Innova 70) with a 5 W maximum power, emitting in 2 dominant wavelengths: green (514.5 nm) and blue (488 nm). Online burst monitoring and processing, using Multi-Bit Fast Fourier Transform, is performed with a burst spectrum analyzer (DANTEC BSA F60). The automatic positioning system has 4 motorized axes, which allows the probe to move along three translation axes and one rotation axis. This configuration offers a fully automatic procedure to carry out the measurement of a whole grid without any human assistance. The measurement grid is located in a plane perpendicular to the turbine axis at the mid height of the distributor. The grid is made of 216 nodes (8 arcs of 27 nodes each). A higher mesh density was adopted near the runner, where more fluctuations are expected as illustrated in figure 3.

In the figure, the mean values of the phase averaged LDV measurements are plotted for each measurement point and the data were interpolated between the original 216 measurement points to render a smoother surface plot.
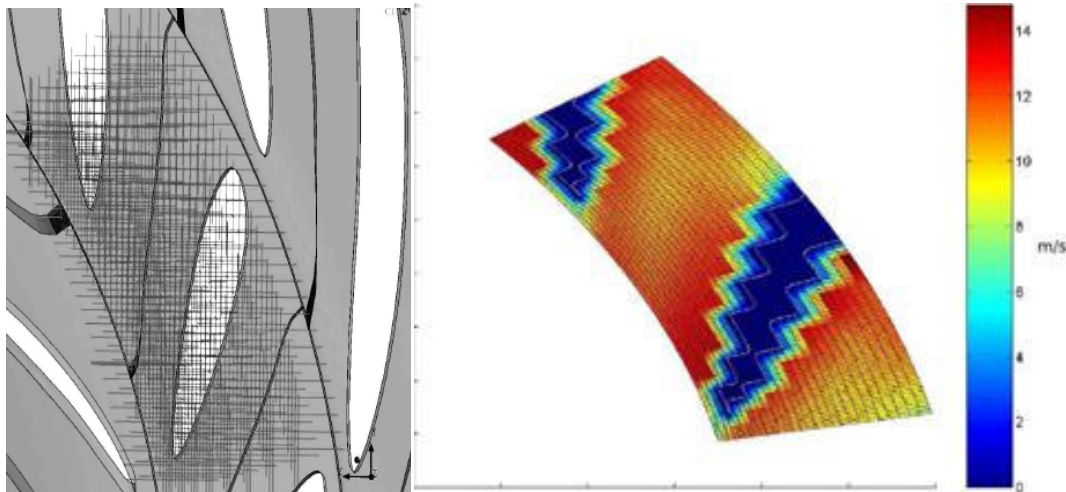

Fig. 3. Position of the laser Doppler velocimetry measurements and corresponding values.

2. Modellization

2.1 Modelling and boundary conditions

The solver Ansys CFX 10 was used for the calculations, running on a 12 CPU cluster at Rainpower, Norway. For setup and post processing, a linux computer with extra memory capacity was used to handle large models.

The inlet boundary condition was set to mass flow, and the outlet condition to average static pressure.

The simulations were run with the k-ε turbulence model, scalable wall functions, high resolution advection scheme and with second order Backward Euler as discretisation algorithm for the transient term. Initial convergence was reached with a frozen rotor simulation prior to starting the transient simulations.

A time step corresponding to a 0.2° runner rotation was used in all simulations with a maximum of three coefficient loop iterations for each time step. The target rms residual was set well below the actual simulation levels, which for all cases was approximately 10^{-5}, so that the cap for maximum number of iterations per time step always was reached. For the last two simulations including draft tube and stay vanes; this gave about five to six minutes of simulation time per time step, running on six dual core CPUs.

2.2 Model 1
The first model, see figure 4, includes the guide vanes and the runner, where the runner domain extended only a fraction of the outlet diameter into the suction cone. Inlet flow angle was set to 20.7 °, similarly to the simulations previously run by B. Nennemann and T.C. Vu [4].

The meshes used for this model were supplied by B. Nennemann and T.C. Vu, GE Hydro, Lachine, Canada. The meshes for the guide vanes and the runner domain were hexa mesh of H-type created with GE Hydro's in house software for structured meshing: X-mesh.

The mesh domain consists of 2.35 million nodes with a mean y^+-value between 100 - 300. The mesh has been created in accordance to GE Hydro's validated methods for meshing, see [1].
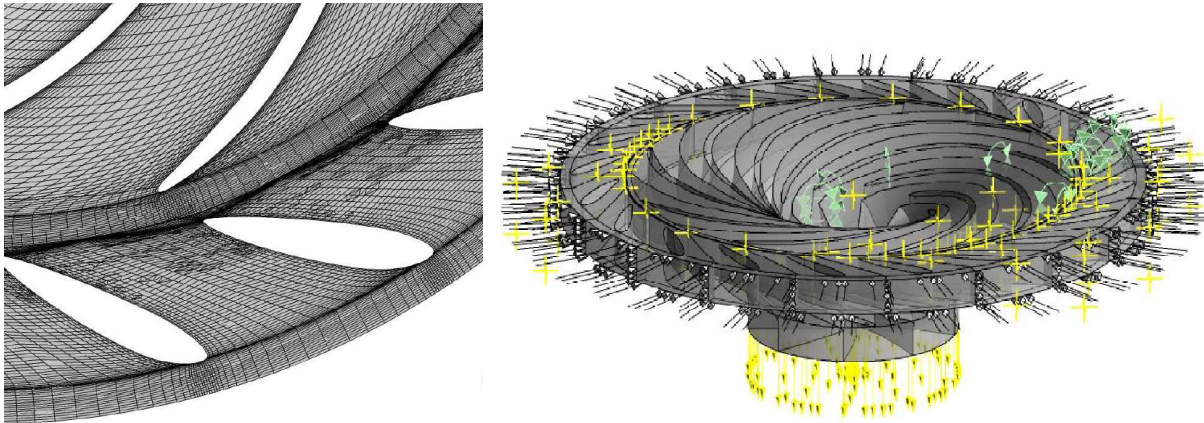

Fig. 4. Model one geometry and X-mesh generated grid for the guide vane and runner domain.

2.3 Model 2
The second model includes the stay vane domain as well as the draft tube. This was done to prevent walls from being placed on the outlet and provide a more realistic inflow condition to the guide vane domain. Since the X-mesh generated guide vane grid had its inlet extended into the theoretical stay vane domain, it was not be possible to add a stay vane domain around it without creating overlapping nodes. This called for a completely new stator mesh including a new guide vane mesh. The new meshes were created in Ansys Turbo Grid 10.0. The stay vane mesh consisted of 50 k nodes and the guide vane mesh of 120 k nodes per blade channel. The guide vane grid was constructed with a higher mesh density to provide for a finer transition from stationary to rotational domain, see figure 6. With a relatively coarse draft tube mesh the total number of nodes in the computational domain was 4.7 million nodes. The simulation was run on six CPUs and needed approximately 5.5 - 6 minutes per time step. The inlet flow angle to the stay vanes was set to 17 °. This angle was approximately measured in the spiral casing from the CAD model. The stator meshes had minimum angles in the range 20-30 ° and produced mean y^+ values around 10 - 40.
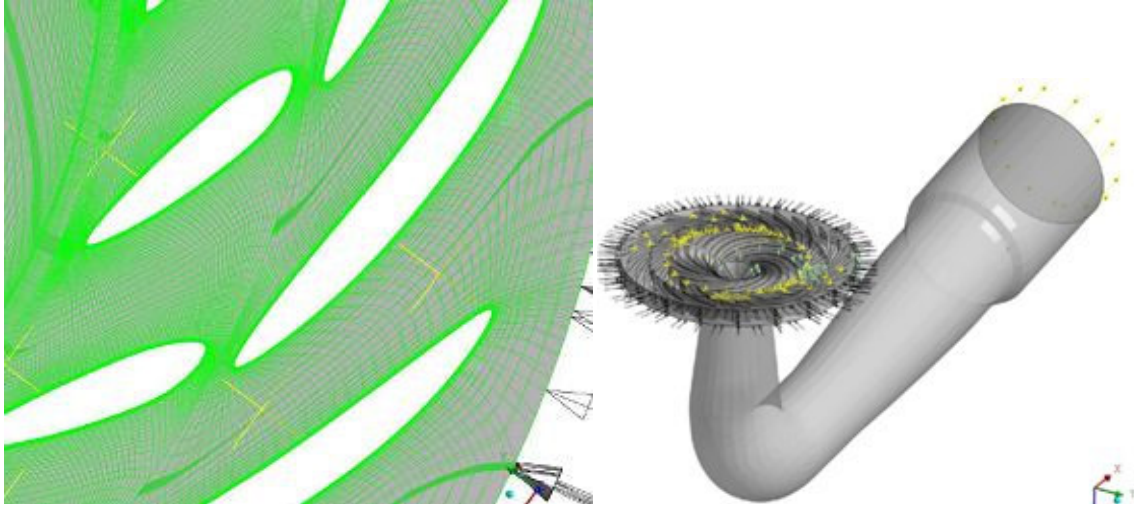
Fig. 5. Model two geometry and mesh generated with Turbo Grid 10.0 grid for the stay vane and runner domain.

2.4 Model 3
The last simulation model was a test to evaluate whether the interface between stator and rotor domain would be better matched if the meshes on both sides of the domain interface were created with the same mesh generator. It was also used to compare two mesh generators. A runner blade mesh was created along with two new stator meshes with emphasis on creating matching node to node conditions between fluid to fluid interfaces. The minimum angle of the runner blade grid was approximately 20 ° and the mean y^+ values ranged from 10 - 40 on the blades throughout the entire computational domain. The runner blade grid consisted of 160k nodes, the guide vane grid of 70k nodes and the stay vane grid of 45k nodes. The mesh is presented in figure 6. The main difference to the X-mesh generated runner grid was larger minimum angles and the absence of a region with elements normal to the rotating domain interface, where the node density is higher, compared with figure 4. The draft tube mesh was the same as the one used in model 2.

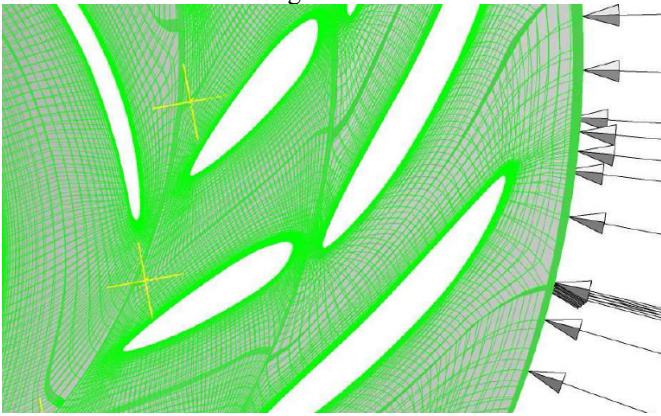The inlet boundary condition was set to 17 ° inflow angle.

Fig. 6. Mesh generated in Turbo Grid at the stay vanes, guide vanes and domain interface to the runner.

3. Results

3.1 Model 1
The Fourier transform of the pressure fluctuations is presented in figure 7. The results indicate that the simulations over predict the results from laboratory measurements by several times, see figure 2 for comparison. The solver placed walls at the outlet, indicating a recirculation region. Tests with adding a draft tube solved the problem with walls at the outlet but did not show significant changes in the pressure fluctuations.

A comparison to LDV measurements, figure 8, showed a large variation of the velocity distribution in the guide vane channel. The variations are attributed to the uniform inlet boundary condition being set too close to the guide vanes. This produced high velocities around the guide vane leading edges that in turn caused the high pressure fluctuations in the runner domain.
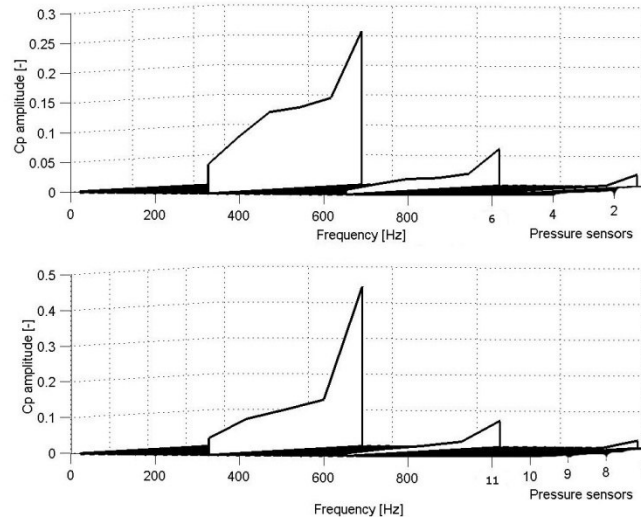

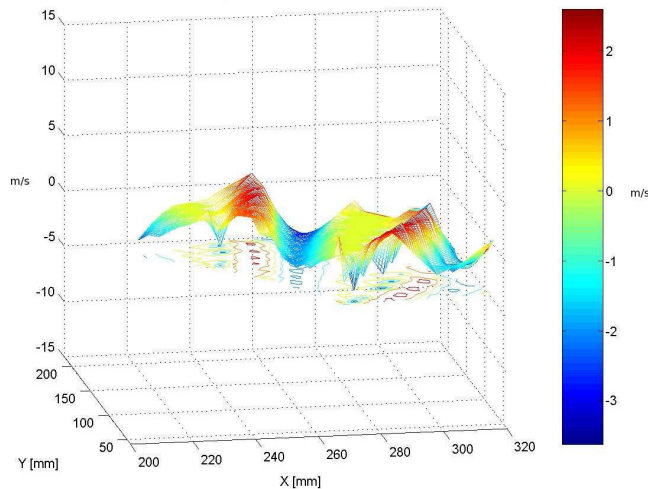**Fig. 7. Waterfall plot of the pressure amplitudes on the pressure (upper) and suction (lower) side using model 1.**

Fig. 8. Difference between simulated and experimental mean velocity for model 1. The regions simulated with high velocity on the outside of the guide vanes can be seen along with regions of low velocity inside of the guide vanes.

3.2 Model 2

The resulting pressure fluctuations from simulations on model 2 are presented in figure 9. In the time domain, the experimental measurements are plotted along with the simulated values for the two pressure sensors on the leading edge of the runner blade. The agreement is good for all pressure sensors except for sensor one on the pressure side, where the readings still were above the experimental predictions.

By adding the draft tube to the computational domain, walls were avoided at the outlet. This however gave rise to a numeric instability that can be seen in the time domain plot of the pressure fluctuations, see figure 9.

In figure 10, the difference between simulated and measured velocities is plotted. Two spikes are seen after the trailing edges of the guide vanes due to a slight difference in the position of the wakes between the experimental and simulated results. The boundary layers are otherwise more evenly reproduced, compared to simulations on model 1.

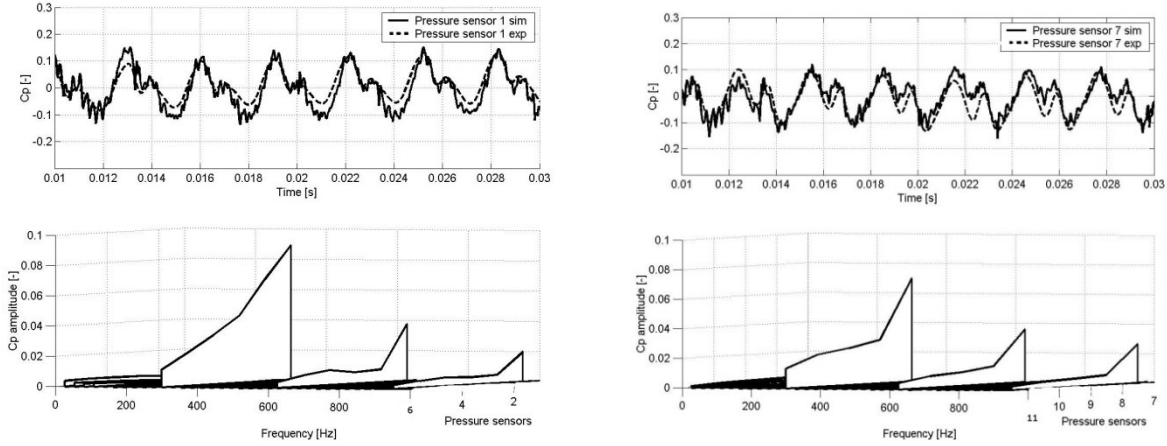Figure 11 show the pressure amplitudes at the guide vane passing frequency compared to experimental results.

Fig. 9. Simulated pressure fluctuations on leading edge sensors on the pressure and suction side and corresponding waterfall plot for model two. The dotted line corresponds to experimental values.
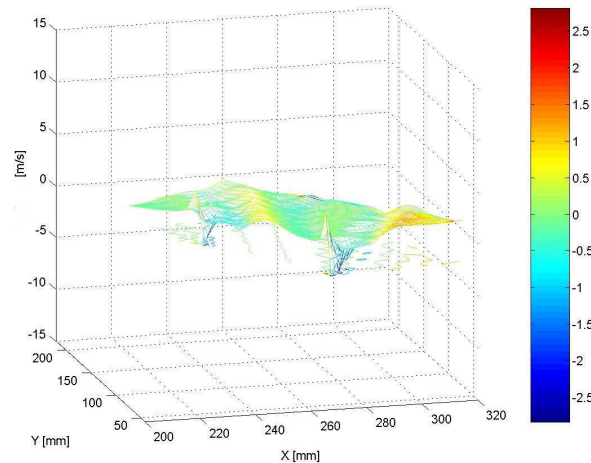

Fig. 10. Difference between the simulated and experimental mean velocity for model 2.
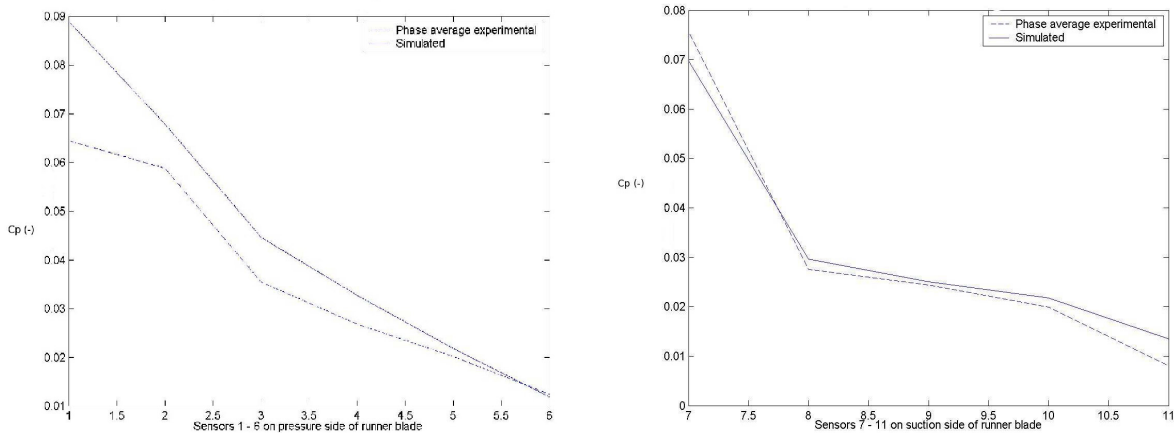

Fig. 11. Experimental and simulated pressure amplitudes at the guide vane passing frequency, pressure and suction side of runner vane.

3.3 Model 3

The results from the simulations are presented in figures 12 and 13. While the velocity field showed a good comparison to the experimental measurements, the waterfall diagrams show that the pressure amplitudes were over predicted. However, the over prediction was mainly located at the first pressure sensors located on the leading edge of the runner blade. In figure 13, describing the difference between simulated and experimental velocity field, two spikes can be seen after the trailing edges of the guide vanes, the same as in the case of model two. The simulated velocity field was relatively well reproduced as a whole in this case with small velocity differences in the guide vane channel.
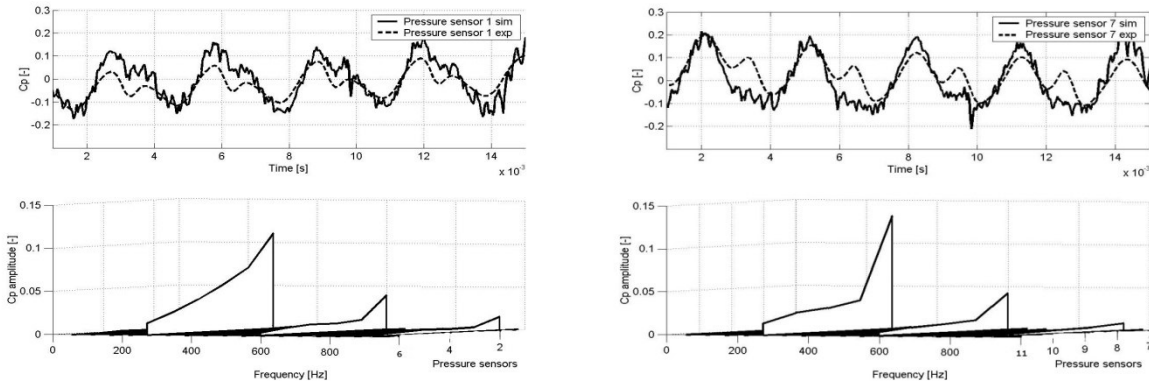

Fig. 12. Simulated pressure fluctuations on leading edge sensors on the pressure and suction side and corresponding waterfall plot for model 3. The dotted line corresponds to experimental values.
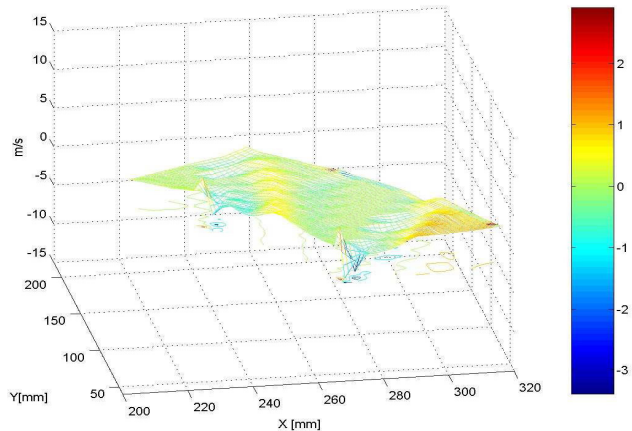

Fig. 13. Difference between experimental and simulated mean velocity for model 3.

4. Discussion

In figure 8, a comparison between simulated and experimental mean velocity shows that the speed of the flow in the outer guide vane boundary layer was under predicted. The cause was attributed to the mean y^+ values, which were rather high (100 – 300) in the first simulation using X-mesh generated grids. A New mesh created with Turbo Grid allowing for a lower value of y+ reproduced the velocity in this region better. The boundary layer flow is however believed to have a relatively small effect for RSI results.

Model 3, with a runner meshed in Turbo Grid, was expected to better reproduce the pressure fluctuations on the runner blade than the simulation on model 2. In this model, a priority was to match nodes on adjacent sides of domain interfaces to each other along the axial direction. This condition was not fulfilled to as high of an accuracy when the grids were constructed in different generators. The results did not match the accuracy of the previous simulation, as shown in figures 9 and 10. This new set up of meshes seems to produce numerical instability to a higher degree than the X-mesh grid. It is believed that this is caused by a difference in meshing at the sliding domain interface. In order to capture the details of the flow when it crosses the domain interface, the grids need to be matched and have a high node density. This is believed to be the reason why the pressure amplitudes on the leading edge of the runner blade were over predicted in the simulation on model 3. The regions, with radial elements,

created for this purpose in X-mesh comes at the expense of mesh minimum angles but seem to do more good than harm, see figure 4.

Another source of error when using Turbo Grid meshes could be differences in volume ratio. Elements close to the inlet and the periodic interfaces of the runner mesh were considerably larger than the average element size, see figure 6. More blocks were added between the runner blade and the periodic interface to improve the mesh quality in this aspect but the problem was only partially solved. In this aspect X-mesh created a higher quality mesh.

5. Conclusions

The investigations of rotor stator interaction on the Hydrodyna pump turbine model, running at full flow rate, using the CFX 10 solver with the $k - \varepsilon$ turbulence model were performed. The pressure amplitudes at the guide vane passing frequency as well as the velocity in a guide vane channel were reproduced with acceptable discrepancy compared to experimental measurements when stay vanes are included in the model. The influence of the draft tube has minor effects on the results, while the choice of mesh generator may influence the results.

References

1. **Nennemann B., Vu T.C., Farhat M.,** "CFD prediction of unsteady wicket gate-runner interaction in Francis turbines: A new standard hydraulic design procedure", Hydro 2005, Villach Austria.
2. **Zobeiri A., Kueny J-L, Farhat M. And Avellan F.,** "Pump-turbine rotor-stator interactions in generating mode: Pressure fluctuation in distributor channel.", IAHR 2006, Toulouse France.
3. **Farhat M., Natal S., Avellan F., Paquet F.,** "Onboard Measurements of Pressure and Strain Fluctuations in a Model of low Head Francis Turbine. Part 1 : Instrumentation". ,IAHR 2002, Lausanne Switzerland
4. **B. Nennemann, T.C. Vu,** "Hydrodyna rotor-stator interaction workshop: Rotor fluctuations." GE Hydro, Lachine, Canada

The Authors

Alf Gunnar Backman He was born in Boden in 1982 (Sweden) and studied at Luleå University of Technology. He obtained in 2008 his M.Sc. in engineering physics. In 2007 he came to Rainpower Norway A.S. to write his master thesis about rotor stator interaction in a pump turbine. In 2008 he started working at the company as Hydraulic Designer.
Jan Tore Billdal gained his PhD in Mechanical Engineering at the Norwegian Institute of Technology in 1987. Between 1986 and 1989 he worked for SINTEF Fluid Machinery where he was Manager for the CFD activity. In 1990 he joined Kvaerner Energy as Senior Research Engineer, Hydraulic Design. Currently he holds the position of Technical Leader, Hydraulic Design, for Rainpower Norway a.s. Since 1996 he has also been Professor (part-time) of Hydraulic Machinery at the Norwegian University of Science and Technology in Trondheim, Norway.
Michel Cervantes received his PhD in 2003 in the field of hydropower at the division of Fluid Mechanics. He has been on academic staff at LTU since this time. He became docent, associate professor, in 2007. His interests are losses, rotor-stator interaction and flow control. He has authored or co-authored over 35 international journal and conference papers in the field of hydropower.
Mohamed Farhat graduated from the Ecole Nationale Supérieur d'Hydraulique et de Mécanique de Grenoble (France) and obtained in 1995 a doctoral degree at Ecole Polytechnique Federale de Lausanne (Switzerland). He joined the R&D department of Hydro Quebec in Montréal (Canada) in 1995 where he was in charge of several research projects in the areas of production and transportation of hydropower and mainly cavitation detection and monitoring in hydraulic turbines. Since 1999, he has been a lecturer and senior scientist at EPFL-LMH laboratory, and head of the cavitation research group.
Ali Reza Zobeiri obtained his master degree in Fluid mechanics in 2001 (Iran). He joined LMH as a doctoral student in 2004 with the objective to work on numerical investigation of rotor-stator interaction in a pump-turbine.